**Physics Journal**
Vol. 1, No. 3, 2015, pp. 272-280
http://www.aiscience.org/journal/pj

# Improved Magnetic Levitation Via Online Disturbance Decoupling

**Timothy Sands***

Department of Mechanical Engineering, Stanford University, Stanford, USA

## Abstract

Control of magnetic levitation systems suffer from coupled physics regardless of control. Feedback control is used to robustly reject disturbances, but is complicated by this coupling. Improved performance is possible by decoupling dynamic disturbance torque, an attractive solution provided by the physics-based control design methodology. Promising approaches include elimination of virtual-zero references, manipulated input decoupling, sensor replacement and disturbance input decoupling. This paper compares the performance of the physics-based control to control methods found in the literature typically including cascaded control topology and neglecting factors such as back-emf.

## Keywords

Physics-Based Controls, Observers, Decoupling, Feedforward, Virtual-Zero References, Luenberger, Gopinath

Received: August 31, 2015 / Accepted: September 16, 2015 / Published online: October 16, 2015



## 1. Introduction

Physics based control is a method that seeks to significantly incorporate the dominant physics of the problem to be controlled into the control design. Some components of the methods include elimination of zero-virtual reference, observers for sensor replacements, manipulated input decoupling, and disturbance-input estimation and decoupling.

## 2. Physics-Based Control

### 2.1. Zero-Virtual References

Zero-virtual references are implicit with cascaded control loops. When inner loops reference signals are not designed otherwise, the cascaded topology results in zero-references, where the inner loop states are naturally zero-seeking. It is generally understood that if any control system demands a positive or negative rate, the inner position loop (seeking zero) would essentially be fighting the rate loop, since a positive or negative rate command with quiescent initial conditions dictates non-zero position command. Elimination of the zero-virtual reference may be accomplished by using analytic expressions for both position and rate eliminating the nested, cascaded topology. Using analytic expressions for both position and rate commands implies the utilization of commands that both correspond to achieving the same desired endstate, essentially eliminating the conflict between the position and rate commands inherit in the cascaded topology.

### 2.2. Sensor Replacement

Due to simplicity of the approach, observer-based augmentation of motion control systems is becoming a ubiquitous method to increase system performance [Ohmae, Matsude, Kaniyama, Tachikawa, 1982], [Yoon, Jung, Too, Sul, 2007], [Yang, Deng, 2005]. The use of observers also permits (in some cases) elimination of hardware associated with sensors, or alternatively may be used as a redundant method to obtain state feedback.

Velocity sensors may be eliminated using speed observers based on position measurement. Estimation is robust to

* Corresponding author
E-mail address: dr.timsands@stanford.edu

parameter variation and sensor noise. Both position and velocity estimates may be used for state feedback eliminating the effects of sensor noise on the state feedback controller.

Luenberger (Figure 1) and Gopinath (Figure 2) observer topologies will be compared. Luenberger-styled observers (henceforth simply referred to as Luenberger observers) are a simple method to estimate velocity given position measurements. Additionally, the Luenberger observer may be used to provide estimates of external system disturbances, since the observer mimics order of actual systems dynamic equations of motion. When used the Luenberger disturbance observer bestows robustness to system parameter variations. Often used terminology is maintained in [Yoon, Jung, Too, Sul, 2007], [Yang, Deng, 2005] where the modification of the signal chosen as the disturbance estimate establishes a "modified" Luenberger observer. The modified Luenberger observer as referred in the cited literature is clearly superior (with respect to disturbance estimation) to the nominal Luenberger observer, so it is assumed to be the baseline Luenberger observer for disturbance estimation.

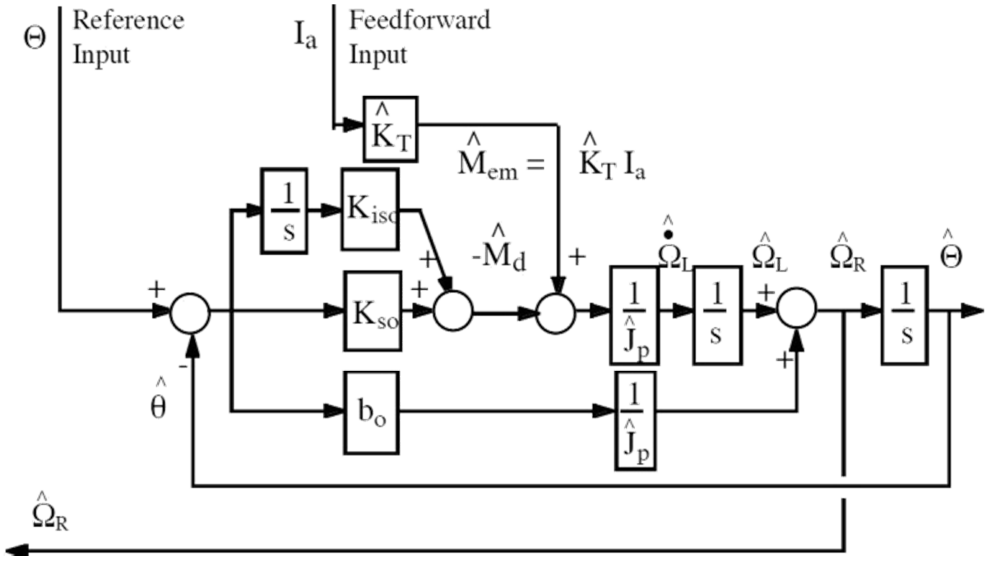


**Figure 1.** Luenberger-Styled Velocity Observer.

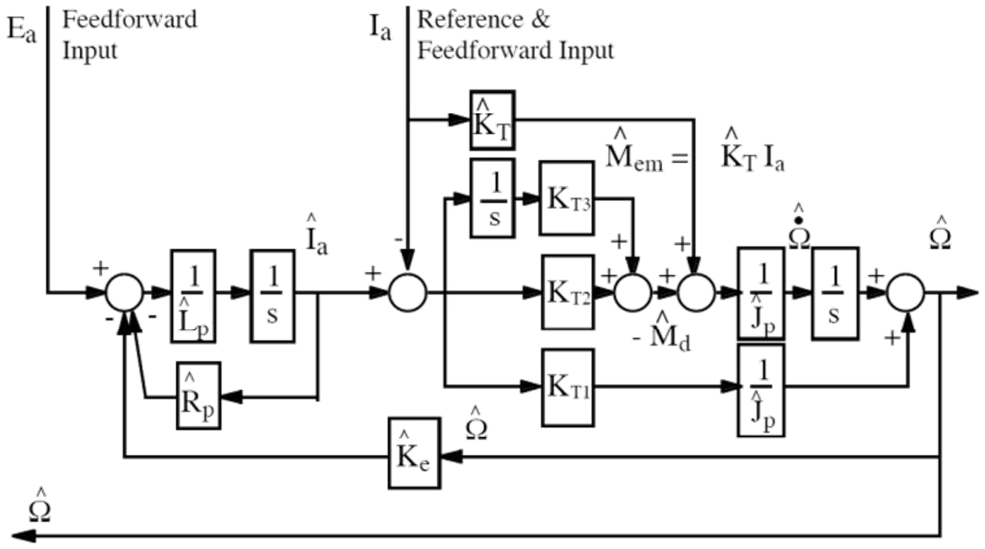


**Figure 2.** Gopinath-Styled Velocity Observer.

References [Yoon, Jung, Too, Sul, 2007], and [Yang, Deng, 2005] improve estimation performance by augmenting the architecture with a second, identical Luenberger observer. The two observers are tuned to estimate velocity and external disturbances respectively. The approach improves estimation accuracy and system performance, but still suffers from estimation lag, so improved methods should be available if estimation lag is eliminated.

Methods to improve estimation performance will be presented. Together with estimation improvement, motion control will be enhanced with disturbance input decoupling (which also aids estimation performance).

### 2.2.1. Manipulated Input Decoupling (MID)

Manipulated input is the actual variable that can be modified by a control design. Very often in academic settings control u is the goal of a design, but in reality a voltage command is sent to a control actuator, and this voltage command should be referred to as the true manipulated input. The importance of this distinction lies in the fact that electronics may not properly replicated the desired control u, unless the control designer has accounted for internal disturbance factors like the resistive effects of back-emf (inherit in any electronic device where current is generated and modified in the presence of a magnetic field). The manipulated input signal should be designed to decouple these effects.

### 2.2.2. Disturbance Input Decoupling (DID)

Augmentation of speed observers with a command feedforward path permits near-zero lag estimation, even in a single-observer topology. Elimination of estimation lag improves estimation accuracy which subsequently improves the performance of the motion controller.

Augmentation of the motion controller with disturbance input decoupling extends the bandwidth of nearly-zero lag estimation considerably again even in a single-observer topology.

The estimates from the observer are frequently used for state feedback eliminating the requirements for both velocity sensors and position measurement smoothing. Adding command feedforward to the observer establishes nearly-zero lag estimation with good accuracy. Furthermore, augmenting the motion controller with disturbance input decoupling improves motion control.

## 3. Zero-Virtual References & MID

Actuators contain electronics that often contain other force or torque motors. Motors associated with electronics are cascaded inner-loops, and they are often paid less attention in the control design. Such cascaded inner loops often reduce the overall system bandwidth due to zero-virtual references. Lacking designed references, the cascaded inner loops seek zero. Design engineers should consider eliminating zero-virtual reference and decoupling the cascaded electronics to increase overall system performance. Consider four voice-coil force actuators (figure 3), and pay particular attention to the fact that force output is coupled due to back-emf and armature resistance which physically desire to seek a virtual-zero reference.

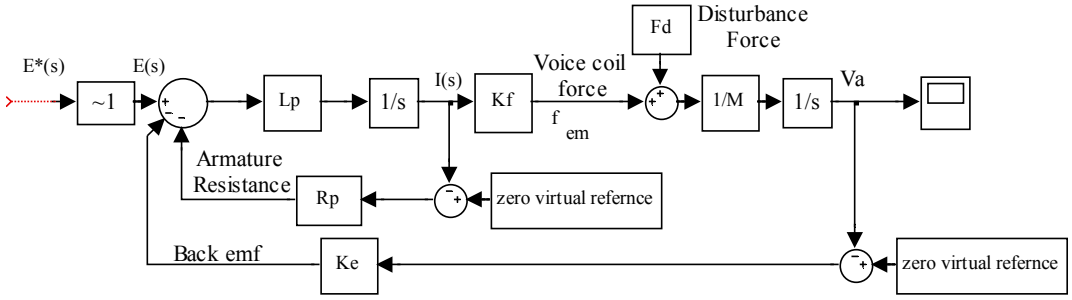


**Figure 3.** Voice coil actuator.

Note the presence of cross coupled armature resistance and back-emf

$$\frac{I(s)}{I^*(s)} = \frac{R_a}{L_p s + R_a + R_p} \rightarrow \frac{R_a}{L_p s + R_a}\bigg|_{\hat{R}_p \rightarrow R_p} \tag{1}$$

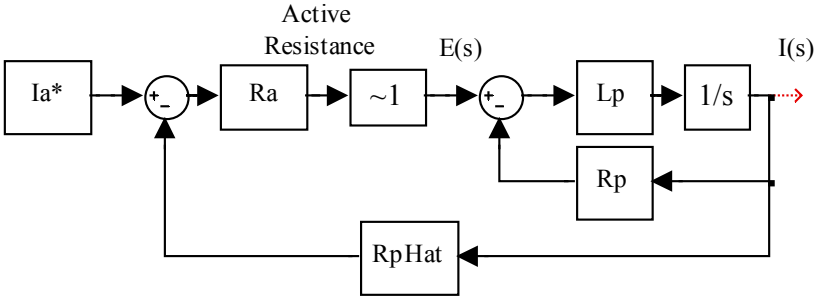


**Figure 4.** Decoupling armature resistance.

An initial goal is to regulate i(t) to regulate fem, (since i(t) and fem are identical variables for this class of machines) to get well-behaved dynamics for the motion states. Since velocity-dependent back-emf complicates the electrical dynamics (it is cross-coupled state feedback), feedback decoupling was implemented. Especially since Ke and Kf are often quite high, back emf can be quite a factor if not dealt with. Note that positive feedback for approximately nulls Ke.

Next, the effects of voice-coil resistance Rp were decoupled (figure 5) with feedback decoupling (i.e. decouple the effects of the armature resistance). Neither of these activities (decoupling back-emf and armature resistance) improves dynamics stiffness rather they yield well behaved force modulators. As a matter of fact, decoupling back-emf results in system inertia being the only remaining system disturbance rejection property.

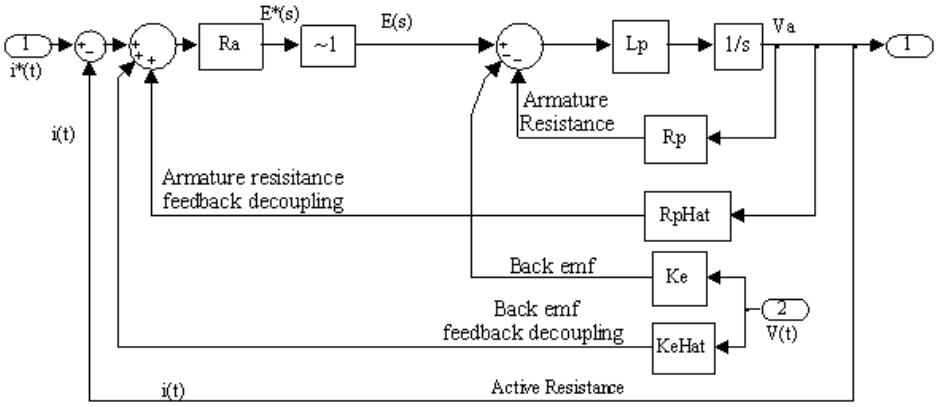


**Figure 5.** Voice coil actuator with decoupling of armature resistance and back-emf.

The figure below (figure 6) is a simplified block diagram that assumes the back-emf and armature resistance have been decoupled (driven to near-zero). Mason's rule analysis (similar to the one done for decoupling armature resistance in figure 4) demonstrates that decoupling yields unity gain current regulators.

Notice this remains strictly true as the armature resistance estimation is accurate. In reality, it is okay if it is not strictly true. The goal is to reduce the effects of armature resistance to allow the active resistance to dominate yielding well-behaved current regulators (i.e. within the regulators bandwidth, the behavior is nearly exactly as desired). Since these are the cascaded low energy states that feed the high energy motion states, the active resistance was tuned to a high bandwidth, 100 Hz (resulting value of Ra=4).

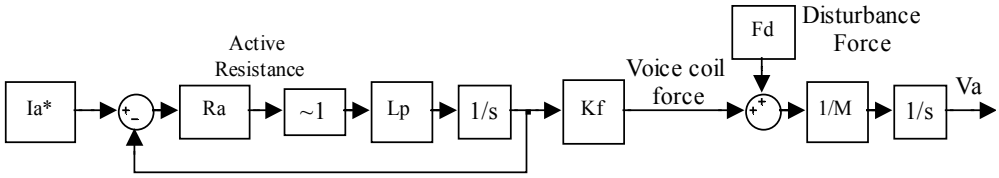


**Figure 6.** Well-behaved force voice-coil actuator.

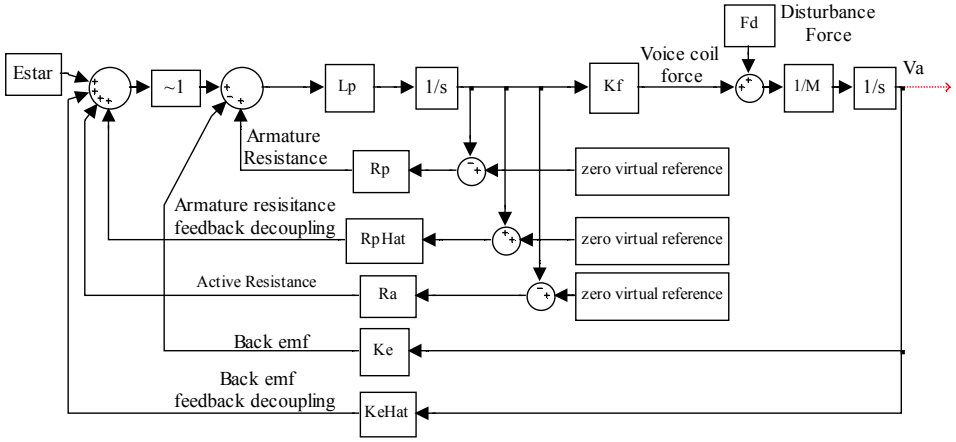


**Figure 7.** Voice-coil state block diagram with virtual-zero reference.

After decoupling back-emf and armature resistance, the now-dominant active resistance that may be tuned for system performance.

Neglecting armature resistance and back-emf decoupling, the resultant dynamic stiffness is:

$$\frac{F_d(s)}{V(s)} = \frac{M_v L_p s^4}{(b_a s^2) + K_{rsas} + K_{risa}(L_p s - R_p)(K_f) + K_e L_p s^4} \quad (2)$$

The effects of decoupling may be observed on dynamic stiffness by setting an terms to zero to expose the individual effects of each loop on disturbance rejection.

## 4. Sensor Replacement: Observers

This section of the paper evaluates the effect of observer types on two, observer-based, incremental motion format, state feedback motion controllers with a cascaded current loop applied to the dc servo drive in Figure 4 with state feedback decoupling, but not disturbance input decoupling (to be performed in a later section of the paper).

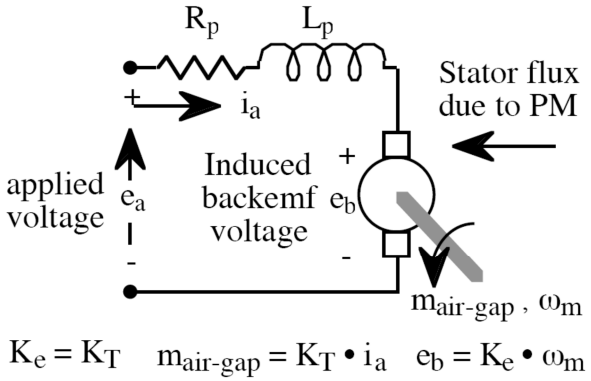


**Figure 8.** DC servo drive (cascaded current loop).

**Table 1.** Parameter Values and Variable Definitions.

| | |
|---|---|
| $J_p$ = 0.015x10-3 Kg-m2 | polar moment of inertia |
| $K_T$ = 0.14 Nm/Amp | torque constant |
| $K_e$ = 0.14 volts/rad/sec | back-emf constant |
| $R_p$ = 2.6 ohms | armature resistance |
| $L_p$ =4.3 milli-henries | armature inductance |
| $e_s$ = applied terminal voltage in volts | |
| $I_a$ = armature current in amperes | |
| $m_{ag}$ = electromagnetic air-gap torque (moment) = $K_T i_a$ | |
| $e_b$ = inducted (back emf) voltage = $K_e \omega_m$ in volts | |
| $\omega_m$ =load angular velocity in rad/sec | |
| $\theta_m$ = load angular position in rad | |

*Part 1 Observer Gain Tuning*

For desired observer eigenvalues $\lambda_1$=12.5, $\lambda_2$=50, $\lambda_3$=200, desired motion controller gains (tuned for disturbance rejection) $\lambda_{c1}$=6, $\lambda_{c2}$=25, $\lambda_{c3}$=100, and current regulator gain $\lambda_i$=800, the general form of the characteristic equation may be equated to the specific observer forms, controller form and current regulator form revealing gains. Tuning was directed in the problem statement to be identical to permit apples-to-apples comparison of effects on estimation accuracy.

Luenberger Tuning (actual current):

$$\text{C.E.} = (s+\lambda_1)(s+\lambda_2)(s+\lambda_3) = \hat{J}_p s^3 + b_o s^2 s + K_{so} s + K_{iso} \quad (3)$$

$$b_o = \hat{J}_p(\lambda_1 + \lambda_2 + \lambda_3) \quad (4)$$

$$K_{so} = \hat{J}_p([\lambda_1(\lambda_2 + \lambda_3) + \lambda_2 \lambda_3] \; K_{iso} = \hat{J}_p(\lambda_1 \lambda_2 \lambda_3) \quad (5)$$

Gopinath Tuning:

$$\frac{\hat{\omega}(s)}{\omega(s)} = \frac{(K_{t1}s^2 + K_{t2}s + K_{t3})\left(\frac{J_p s^2(L_p - \hat{L}_p) + J_p(R_p - \hat{R}_p)s}{K_t} + \frac{\hat{K}_t}{K_t} J_p s(\hat{L}_p + \hat{R}_p)\right)}{\hat{J}_p \hat{L}_p s^3 + (\hat{J}_p R_p + \hat{K}_e K_1)s^2 + \hat{K}_e K_2 s + \hat{K}_e K_3} \quad (6)$$

Equating coefficient of 's' and solve for gains:

$$(s+\lambda_1)(s+\lambda_2)(s+\lambda_3) = \hat{J}_p s^3 + (\hat{J}_p \hat{R}_p + \hat{K}_e K_1)s^2 + \hat{K}_e K_2 s + \hat{K}_e K_3 \quad (7)$$

$$K_1 = \frac{\hat{J}_p \hat{L}_p(\lambda_1 + \lambda_2 + \lambda_3) - \hat{J}_p \hat{R}_p}{\hat{K}_e} \quad (8)$$

$$K_3 = \frac{\hat{J}_p \hat{L}_p}{\hat{K}_e}(\lambda_1 \lambda_2 \lambda_3) \quad (9)$$

$$K_2 = \frac{\hat{J}_p \hat{L}_p(\lambda_1 \lambda_2 + \lambda_3) - \hat{J}_p R_p(\lambda_1(\lambda_2 + \lambda_3) + \lambda_2 \lambda_3)}{\hat{K}_e} \quad (10)$$

*Motion Controller:*

$$(s+\lambda_{c1})(s+\lambda_{c2})(s+\lambda_{c3}) = \hat{J}_p s^3 + b_a s^2 s + K_s s + K_{is} \quad (11)$$

$$\textit{Current regulator}: (s+\lambda_i) = L_p s + R_a \quad (12)$$

While the Luenberger observers diverge very close to the maximum tuned bandwidth (even with parameter errors), the Gopinath observer diverges at a lower bandwidth when errors are present. Since both observers contain a current-feedforward element, you will see nearly zero-lag properties out to the bandwidth of the feedback observer controller. Clearly, disturbances (in the form of modeling errors here) do not influence low frequency estimation (likely due to the addition of integrators in the observer controllers). The Gopinath observer was particularly sensitive to errors in Kt indicating its reliance on the feedforward estimation path.

Notice in particular in Figure 10 that zero-lag estimation occurs even with inaccurate Kt (albeit with non-zero estimation frequency response at all frequencies).

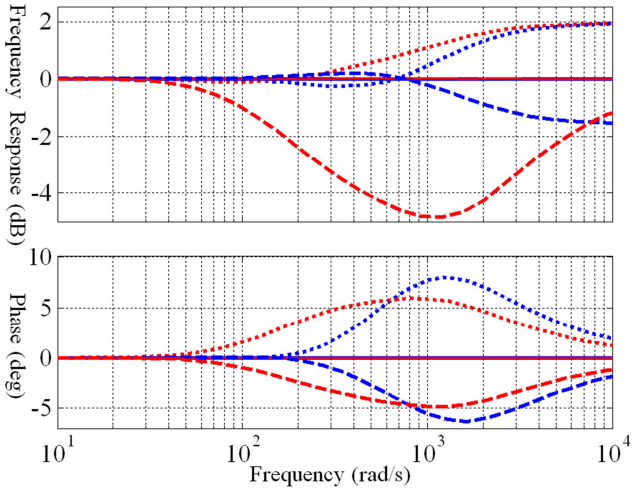


**Figure 9.** Comparison of estimation accuracy frequency response functions for incorrect Jp^ . Luenberger (blue) Gopinath (red); dotted = -20% error, solid = 0% error; dashed = +20% error.

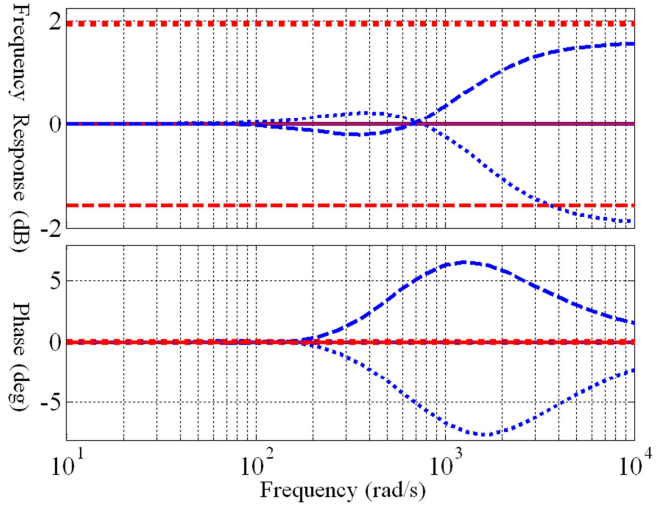


**Figure 10.** Comparison of estimation accuracy frequency response functions for incorrect Kt=Ke. Luenberger (blue) Gopinath (red); dotted = -20% error, solid = 0% error; dashed = +20% error.

One suggestion for improved command tracking is to remove feedback decoupling as done here replacing it with feedforward decoupling permitting the disturbance torque to excite the decoupling. One other thing: Note the maximum phase lag of 90 degrees. Such a maximum would be expected in a system with a command feedforward control scheme. Since the feedforward path would remain nearly zero-lag, the 90-degree phase lag would be creditable to Shannon's sampling-limit theory. Since there is no command feedforward control in this scheme, the lack of a maximum phase shift of 180 degrees (for a double integrator plant) is puzzling.

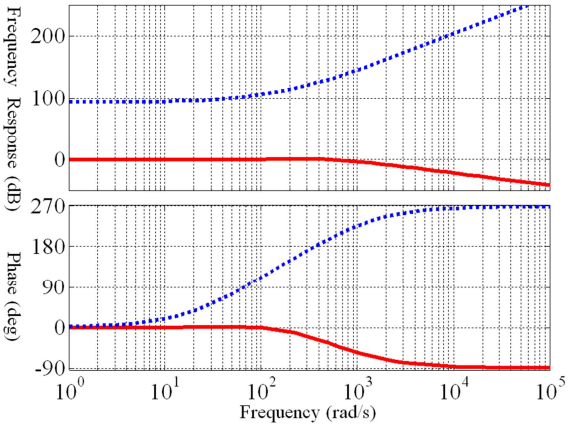


**Figure 11.** Frequency Response Functions for the motion control system.

Observer tuning (not the current loop tuning) determines the maximum frequency for nearly zero-lag accurate estimation. Since the commanded and actual current are nearly identical (also with zero lag) out to the higher current loop bandwidth, it was expected that the effects of commanded versus actual current are mitigated by feedback decoupling (i.e. we exceed the observer bandwidths before there is an appreciable difference in commanded versus actual current).

Actually, the Luenberger observer was sensitive to output noise associate with actual current. The noisier actual current signal does not pass through a smoothing integrator before going directly into the plant dynamics. On other hand, the Gopinath observer compares the estimated and actual/commanded current (i.e. current estimation error) through a smoothing integrator in the observer controller and also passes a portion through a separate smoothing integrator associate with angular rate estimation. Thus, the Gopinath-styled observer was insensitive to commanded versus measured current due to feedback decoupling. The Luenberger observer may be made less sensitive to the difference between commanded and actual current (and other system noises and errors) by using the actual rotation angle as input to the observer (Figure 13). As a matter of fact, this iteration resulted in the best performance for the evaluated case of sinusoidal sensor noise demonstrating the least mean error.

## 5. Disturbance Input Decoupling

This paragraph reformulates the Yoon paper's dual observer-based DID system consistent with physics-based control methods and furthermore evaluates opportunities in the proposed structure. Physics-based methods recommend 1) disturbance input decoupling followed by 2) state feedback decoupling of system cross-coupling, then 3) elimination of virtual zero references, then finally adding active state

feedback with full state references. Note the observer structure is different with added command feedforward shown in Figure 12 & Figure 13.

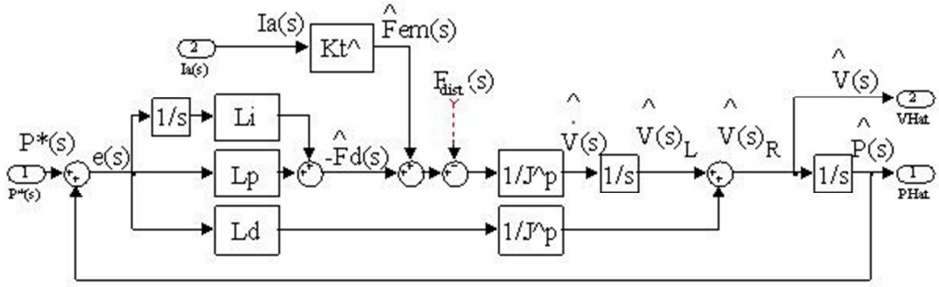


**Figure 12.** Luenberger-styled observer with command feedforward.

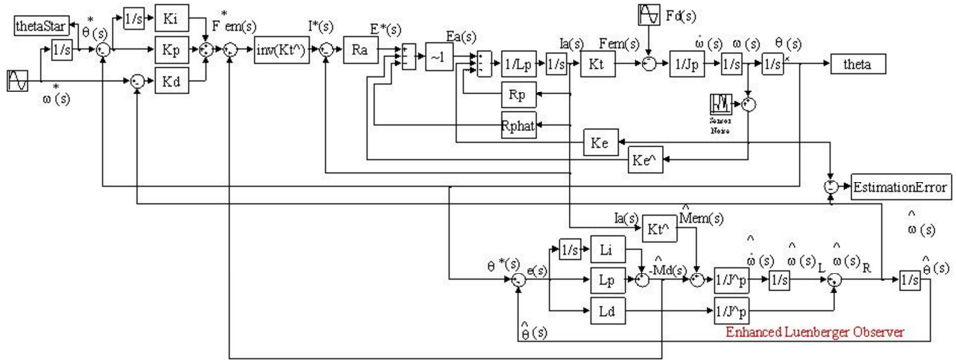


**Figure 13.** Decoupled motion control w/DID & Luenberger observer with command feedforward.

Emphasize velocity estimation for state feedback of motion controllers. The improvements achieve near-zero lag, accurate velocity estimation as displayed in Figure 16 and Figure 17 for clarity. The larger scale of Figure 17 reveals the advantages over the most recently proposed improved methods. High-frequency roll-off is drastically improved by addition of command feedforward (of the true manipulated input) to the Luenberger observer. Additional inclusion of disturbance input decoupling in the motion control system improves velocity estimates in the observer, essentially eliminating roll-off and estimation lag. This later claim is more clearly displayed in the zoomed response plot in Figure 16.

The cascaded control topology should be eliminated adding full command references. Command feedforward control should be added. The electro-dynamics should not be ignored in the analysis. It causes the illusion that force is the manipulated input as opposed to current (the true manipulated input) resulting in lower bandwidth. Neglecting the electrodynamics results in an analysis that is inadequately reinforces the experiments. Yoon refers to "disturbances forces generated by the current controller" to explain the difference between experimentation and analysis. Decoupling the electro-dynamics will improve performance even without full command references. Without manipulated input decoupling (MID), you have an implied zero-reference command for current. Assuming an inductor motor's electronics, decoupling Ke should dramatically increase disturbance rejection isolating the electrical system. The paper utilizes a dual observer to permit individual tuning for disparate purposes (DID and velocity estimation), but then implies using identical observer gains! That makes no sense. Instead of using identical gains, eliminate one of the observers to simplify the algorithmic complexity. Alternatively, utilize different gains optimized respectively for velocity and disturbance estimation. A first step for comparison requires repetition of the Yoon paper results. Equations (3), (4), and (5) in the Yoon paper are plotted in Figure 14, which should duplicate figure (5) in the Yoon paper. Note the slightly different result was achieved only in the case of modified observer (not the proposed dual-observer method).

Next, equations (6), (7), and (8) in the Yoon paper were plotted in Figure 15, which duplicates Yoon's figure 6. Again, notice a slight difference this time with the estimation FRF of the basic Luenberger observer. According to the paper's plots in figure 6, the modified observer estimates more poorly than the nominal observer by dramatically overestimating velocity. This clearly indicates a labeling-error in the paper's figure. Also, the Luenberger observer does not estimate well within the observer bandwidth, so my results displayed here seems more credible. The difference is negligible considering the performance to be gained using physics-based reformulation.

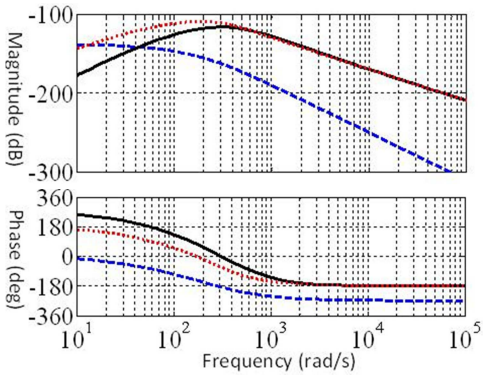


**Figure 14.** Nominal response comparison: Solid-black line is Luenberger observer; Blue-dashed line is Modified Luenberger observer; Red-dotted line is no compensation.

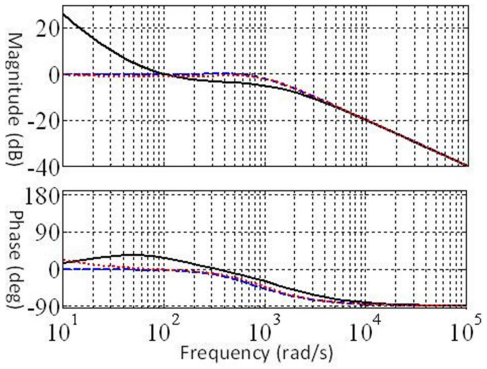


**Figure 15.** Response comparison: Solid-black line is Luenberger observer; Red-dotted line is Modified Luenberger observer; Blue-dashed line is Dual Observer.

The reformulation results in the estimation FRF with DID and command feedforward is displayed Figure 16 & Figure 17. Immediately notice that addition of the command feedforward to the modified Luenberger observer yields nearly-zero lag estimates, far superior to the Yoon paper (which omitted the command feedforward path in what they call an observer). It is a premise of the physics-based methodology that the title "observer" implies nearly-zero lag estimation, so one might argue that the Yoon paper really utilizes a state filter rather than a state observer.

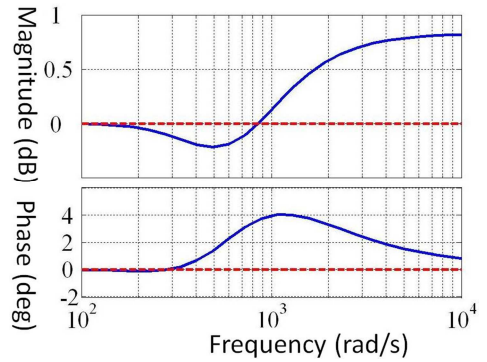


**Figure 16.** Observer Improvements estimation comparison: Solid-blue line is Modified Luenberger observer with command feedforward; Red-dashed line is Modified Luenberger observer with command feedforward and disturbance input decoupling.

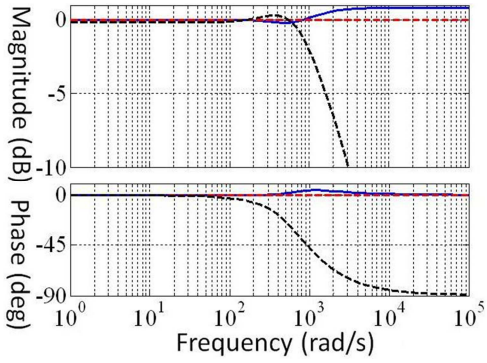


**Figure 17.** Observer Improvements estimation comparison: Solid-blue line is Modified Luenberger observer with command feedforward; Red-dashed line is Modified Luenberger observer with command feedforward and disturbance input decoupling; Dashed-black line is Dual Observers.

The results using the physics-based methodology are clearly superior despite relative algorithmic simplicity. Adding the command feedforward permits accurate, near-zero lag estimation of velocity without a velocity sensor. Furthermore, disturbance input decoupling increases system robustness and permits accurate estimation inaccuracy even when unknown disturbances are present. Certainly, accounting for the electrodynamics should always be done rather than neglecting them as "system noise" as done in the Yoon paper.

$$F_{dist} = [P(s)-P(s)]\left[K_d s+K_p+\frac{K_i}{s}\right] = \frac{s^2\left[\hat{P}(s)-P(s)\right]\left[K_d s+K_p+\frac{K_i}{s}\right]}{s^2} = \frac{\left[\hat{V}(s)-V(s)\right]\left[K_d s+K_p+\frac{K_i}{s}\right]}{s^2} \quad (13)$$

$$\hat{V}(s)\left[1+\frac{L_d}{\hat{M}}\frac{1}{s}+\frac{L_p}{\hat{M}}\frac{1}{s^2}+\frac{L_i}{\hat{M}}\frac{1}{s^3}\right] = V(s)\left[\frac{\hat{K}_T}{K_T}\frac{M}{\hat{M}}+\frac{L_d}{\hat{M}}\frac{1}{s}+\frac{L_p}{\hat{M}}\frac{1}{s^2}+\frac{L_i}{\hat{M}}\frac{1}{s^3}\right] + \left[\hat{V}(s)-V(s)\right]\left[K_d+\frac{K_p}{s}+\frac{K_i}{s^2}\right] \quad (14)$$

$$\hat{V}(s)\left[1+\frac{L_d}{\hat{M}}\frac{1}{s}+\frac{L_p}{\hat{M}}\frac{1}{s^2}+\frac{L_i}{\hat{M}}\frac{1}{s^3}-K_d-\frac{K_p}{s}-\frac{K_i}{s^2}\right] = V(s)\left[\frac{\hat{K}_T}{K_T}\frac{M}{\hat{M}}+\frac{L_d}{\hat{M}}\frac{1}{s}+\frac{L_p}{\hat{M}}\frac{1}{s^2}+\frac{L_i}{\hat{M}}\frac{1}{s^3}-K_d-\frac{K_p}{s}-\frac{K_i}{s^2}\right] \quad (15)$$

Multiplying by $s^3$:

$$\hat{V}(s)\left[s^3+\frac{L_d}{\hat{M}}s^2+\frac{L_p}{\hat{M}}s+\frac{L_i}{\hat{M}}-K_d s^3-K_p s^2-K_i s\right] = V(s)\left[\frac{\hat{K}_T}{K_T}\frac{M}{\hat{M}}s^3+\frac{L_d}{\hat{M}}s^2+\frac{L_p}{\hat{M}}s+\frac{L_i}{\hat{M}}-K_d s^3-K_p s^2-K_i s\right] \quad (16)$$

$$\frac{\hat{V}(s)}{V(s)} = \frac{\left[\frac{\hat{K}_T}{K_T}\frac{M}{\hat{M}} - K_d\right]s^3 + \left[\frac{L_d}{\hat{M}} - K_p\right]s^2 + \left[\frac{L_p}{\hat{M}} - K_i\right]s + \frac{L_i}{\hat{M}}}{\left[1 - K_d\right]s^3 + \left[\frac{L_d}{\hat{M}} - K_p\right]s^2 + \left[\frac{L_p}{\hat{M}} - K_i\right]s + \frac{L_i}{\hat{M}}} \quad (17)$$

## 6. Conclusions

Physics based control is a method that seeks to significantly incorporate the dominant physics of the problem to be controlled into the control design. Some components of the methods include elimination of zero-virtual reference, observers for sensor replacements, manipulated input decoupling, and disturbance-input estimation and decoupling. Decoupling dynamic disturbance torques is an attractive solution provided by the physics-based control design methodology. This paper compares the performance of the physics-based control to control methods found in the literature typically including cascaded control topology and neglecting factors such as back-emf.

Recommendation: Use enhanced Luenberger-styled observers w/actual θ(s) for such plants.

## Acknowledgement

For inspiring this research special thanks go to R. D. Lorenz, Consolidated Papers Professor of Controls Engineering at the University of Wisconsin at Madison.

## References

[1] Kempf, C. J. and S. Kobayashi, “Disturbance observer and feedforward design of a high-speed direct-drive positioning table”, IEEE Trans. On Control Systems Tech., vol. 7, no. 5, Sep., 1999.

[2] Kim, J. K., J. W. Choi, and S. K. Sul, “High performance position control of linear permanent magnet synchronous motor for surface mount device in placement system,” in Conf. Rec. PCC-Osaka, vol. 1, 2002, pp. 37-42.

[3] Liu, M. Z., T. Tsuji, and T. Hanamato, “Position control of magnetic levitation transfer system by pitch angle,” Journal of Power Electronics, vol. 6, no. 3, July 2006.

[4] Ohmae, T., T. Matsuda, K. Kaniyama, and M. Tachikawa, “A microprocessor-controlled high-accuracy wide-range speed regulator for motor drives,” IEEE Trans. on Ind. Electron., vol. 29, no. 3, August, 1982.

[5] Tan, K.K., T. H. Lee, H. F. Dou, S. J. Chin, and Shao Zhao, “Precision motion control with disturbance observer for pulsewidth-modulated-driven permanent-magnet linear motors,” IEEE Trans. on Magnetics, vol. 39, no. 3, May, 2003.

[6] Tesfaye, A., H. S. Lee and M. Tomizuka, “A sensitivity optimization approach to design of a disturbance observer in digital motion control systems”, IEEE/ASME Trans. on Mechatronics, vol. 5, no. 1, March, 2000.

[7] Yang, S. M., and Y. J. Deng, “Observer-based inertia identification for auto-tuning servo motor-drives”, in Industry Applications Conference, vol. 2, 2005, pp. 968-972.

[8] Yoo, A., Y. D. Yoon, S. K. Sul, M. Hisatune, and S. Morimoto, “Design of a current regulator with extended bandwidth for servo motor drive,” in Conf. Rec. PCC-Nagoya, 2007.

[9] Yoon, Y. D., E. Jung, A. Yoo, and S. K. Sul, “Dual observers for the disturbance rejection of a motion control system,” in Conf. Rec. 42nd IAS Annual Meeting, 2007, pp. 256-261.

[10] Topographies taken from ME746 course notes, University of Wisconsin at Madison.